Direct writing and characterization of poly(p-phenylene vinylene) nanostructures

Debin Wang, Suenne Kim, William D. Underwood, Anthony J. Giordano, Clifford L. Henderson et al.

Additional information on Appl. Phys. Lett.
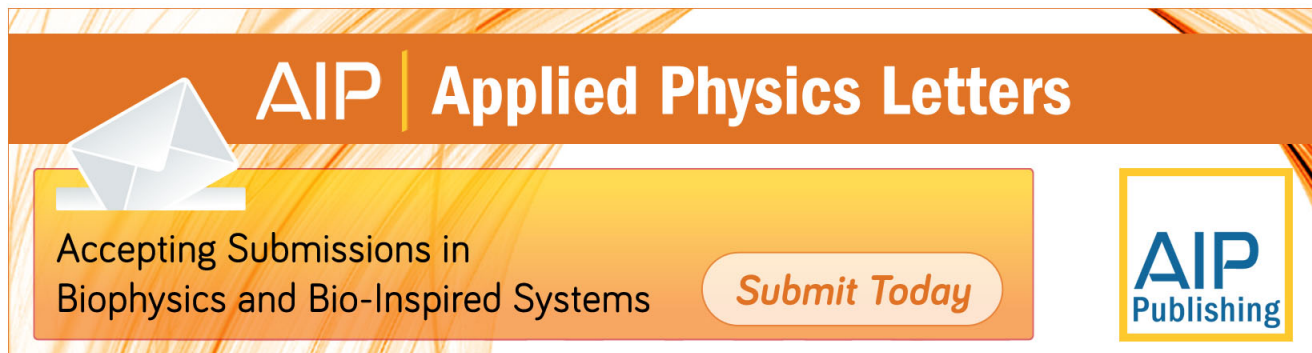
Direct writing and characterization of poly(*p*-phenylene vinylene) nanostructures

Debin Wang,[1] Suenne Kim,[1] William D. Underwood II,[2] Anthony J. Giordano,[2] Clifford L. Henderson,[3] Zhenting Dai,[4] William P. King,[4] Seth R. Marder,[2] and Elisa Riedo[1,a)]

[1]*School of Physics, Georgia Institute of Technology, Atlanta, Georgia 30332, USA*
[2]*School of Chemistry and Biochemistry, Georgia Institute of Technology, Atlanta, Georgia 30332, USA*
[3]*School of Chemical and Bimolecular Engineering, Georgia Institute of Technology, Atlanta, Georgia 30332, USA*
[4]*Department of Materials Science and Engineering, University of Illinois Urbana-Champaign, Urbana, Illinois 61801, USA*

We report the use of thermochemical nanolithography to convert a precursor polymer film to poly(*p*-phenylene vinylene) with sub-100 nm spatial resolution, in ambient conditions. The local thermochemical conversion is verified by Raman spectroscopy, fluorescence imaging, and atomic force microscopy. This convenient direct writing of conjugated polymer nanostructures could be desirable for the design and fabrication of future nanoelectronic, nanophotonic, and biosensing devices. © *2009 American Institute of Physics*. [doi:10.1063/1.3271178]

Conjugated polymers have been recognized as promising candidates to replace conventional inorganic semiconductor materials in certain electronic and optoelectronic applications.[1] These polymers show many useful optoelectronic properties, such as electroluminescence,[2] high charge carrier mobilities,[3] and photovoltaic effect.[4] Nanopatterning and nanofabrication of conjugated polymers on various length scales have attracted considerable interest for nanoelectronics, nanophotonics, and biosensing. Among the methods that have been reported to date for the patterning of conjugated polymers are electrodeposition,[5] electrospinning,[6] inkjet printing,[7] nanoimprint lithography,[8] dip-pen nanolithography through electrostatic interaction or electrochemical reaction,[9,10] scanning near-field optical lithography,[11,12] thermochemical nanopatterning,[13] and edge lithography.[14]

Thermochemical nanolithography (TCNL) is a versatile technique that allows for control of the local chemistry of thin polymer films. The technique enables the fabrication of one-dimensional or two-dimensional nanostructures with controlled dimensions and positioning. TCNL has been demonstrated to allow for patterning of sub-15 nm features by inducing thermally activated chemical reactions using a heated AFM tip at a speed above 1 mm/s.[15] TCNL can be performed in various environments and can be easily adapted to a variety of substrates and chemical functionalities.[16,17]

This letter reports the direct writing of nanostructures of poly(*p*-phenylene vinylene) (PPV), a widely studied electroluminescent conjugated polymer, by locally heating a sulfonium salt precursor, poly(*p*-xylene tetrahydrothiophenium chloride). Such a thermochemical local conversion route is realized by locally heating in ambient conditions with a resistively heated AFM probe at 240 °C. The precursor thin film is obtained by drop-casting on a glass or silicon (111) substrate.

The PPV was obtained by pyrolysis of a sulfonium salt precursor poly(*p*-xylene tetrahydrothiophenium chloride)

(0.25 wt % in H_2O, Aldrich). The precursor solution was drop cast on either glass slides or Si (111) wafers that had been immersed overnight in a piranha solution. The thermal conversion to PPV typically involves the elimination of both thiophene and hydrogen chloride in inert gas conditions or in vacuum at heating temperatures in the range of 250–300 °C.[1]

Heatable AFM tips were mounted into commercial AFMs (Multimode IV, Veeco and PicoPlus, Molecular Imaging). By applying a direct current bias across the cantilever legs, the temperature at the tip-polymer interface can be controlled and calibrated as described in literature.[16,18] Ultrasharp tapping mode AFM tips (SSS-NCHR, Nanosensors) were used to acquire high resolution topographical images of the PPV nanostructures written by TCNL.

Fluorescence imaging is a convenient method to follow the thermal conversion of a precursor to PPV because of its broad emissive photoluminescence spectrum in the green color region. PPV nanostructures were imaged using fluorescence microscopy with an inverted Nikon TE2000 equipped with a high-sensitivity charge coupled device camera (CoolSNAP HQ2, Roper Scientific). Images were obtained using a Plan Apo 60× water immersion objective (Nikon, NA 1.2). A Nikon filter cube set was used to image fluorescent PPV nanostructures in the green region (#96320, FITC/GFP HyQ filter set, excitation 460–500 nm, dichroic mirror DM505, and emission 510–560 nm). All the Raman data of the present work were obtained from a confocal Raman microscope (Jobin Yvon HR800) using a laser excitation wavelength of 785 nm with the same acquisition time.

Figure 1 shows fluorescence and AFM topography images of the PPV lines made by TCNL. These nanostructures were made at a writing speed of 20 μm/s, with a normal load of 30 nN, and cantilever temperature ranging between 240 and 360 °C. The nanostructures started to show a visible fluorescent contrast at 240 °C. The contrast became clearer as the heating temperature was raised to 360 °C. The corresponding AFM topography image reveals TCNL capability

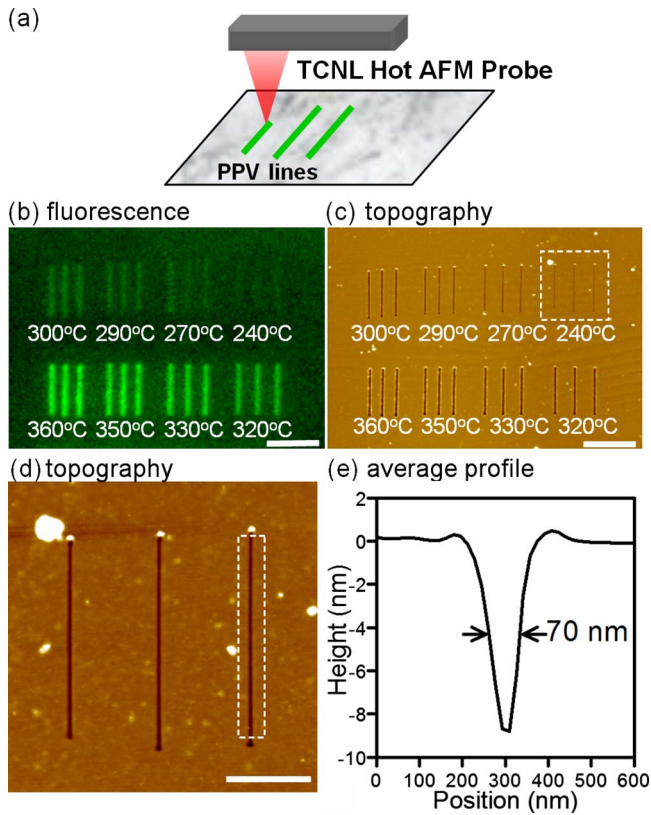a)Electronic mail: elisa.riedo@physics.gatech.edu.

FIG. 1. (Color online) TCNL nanolithography of PPV nanostructures. (a) Scheme of TCNL nanolithography of PPV nanostructures. (b) Fluorescence and (c) AFM topography images of PPV nanostructures made by TCNL at a range of temperatures, 240–360 °C. A zoom-in view of PPV lines made at 240 °C as outlined in (c) is shown in (d). (e) The average profile of the PPV trench outlined in (d) shows that the width (full width at half maximum) of the line is as narrow as 70 nm. The thickness of this precursor film is 100 nm. Scale bars: (b) and (c): 5 μm, (d): 2 μm.

of fabricating PPV nanostructures with a high spatial resolution of 70 nm.

Raman spectroscopy measurements provided more definitive evidence of the thermal conversion and highlighted the quality of the TCNL prepared nanostructures. We produced 20×20 μm^2 TCNL patterns at 240, 280, and 320 °C, with a normal load of 30 nN and a speed of 20 μm/s. Raman measurements revealed that the quality of the PPV patterns formed by TCNL in ambient conditions is comparable to the quality of a PPV sample prepared by a standard thermal annealing of a precursor polymer in vacuum conditions, here referred to PPV$_{reference}$.[19] Raman spectra were obtained from four representative samples: an untreated precursor film in Fig. 2(a), a PPV reference film in Fig. 2(b), a TCNL pattern in Fig. 2(c), and a precursor film bulk heated with a hot plate in air at 280 °C for about an hour in Fig. 2(d). The four samples were obtained from the same precursor polymer batch and had a thickness of 1.4 μm. The PPV$_{reference}$ film was prepared by annealing the precursor film for five hours at 280 °C in a vacuum of ~200 mTorr. The most distinctive characteristics of the Raman spectra after the complete conversion of the precursor film into PPV is the large intensity enhancement [see Figs. 2(a) and 2(b)], which we attribute to a density increase in the polymer film due to a volume contraction.[19] The Raman spectrum of the TCNL pattern in Fig. 2(c) clearly shows the same enhancement in intensity throughout the spectrum. In the case of an ambient bulk
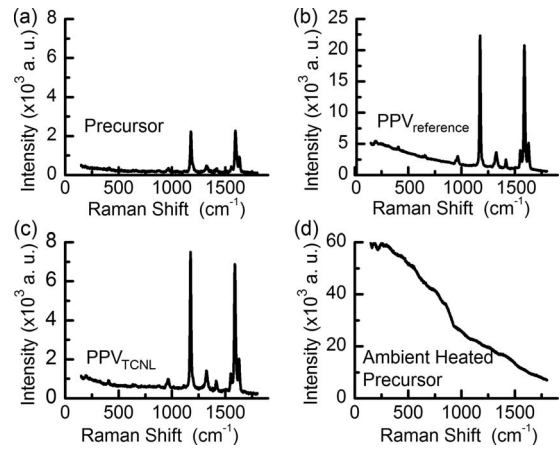

FIG. 2. Raman spectra of (a) untreated precursor, (b) PPV reference, (c) TCNL PPV pattern, and (d) precursor annealed in ambient condition.

heated precursor polymer, as shown in Fig. 2(d), we observe a large continuum background very likely generated by oxidation and the disappearance of the PPV Raman peaks.

Another signature of the precursor-PPV conversion is the shift in frequency of the Raman peaks associated with the C–C vibrations to lower frequencies. With respect to the PPV$_{reference}$, the two Raman peaks of the untreated precursor polymer at around 1178 and 1594 cm^{-1} are found to shift by 3 and 6 cm^{-1}, respectively, after the conversion as depicted in Fig. 3(a). The Raman peak positions of the TCNL patterns written at three different tip temperatures are in between
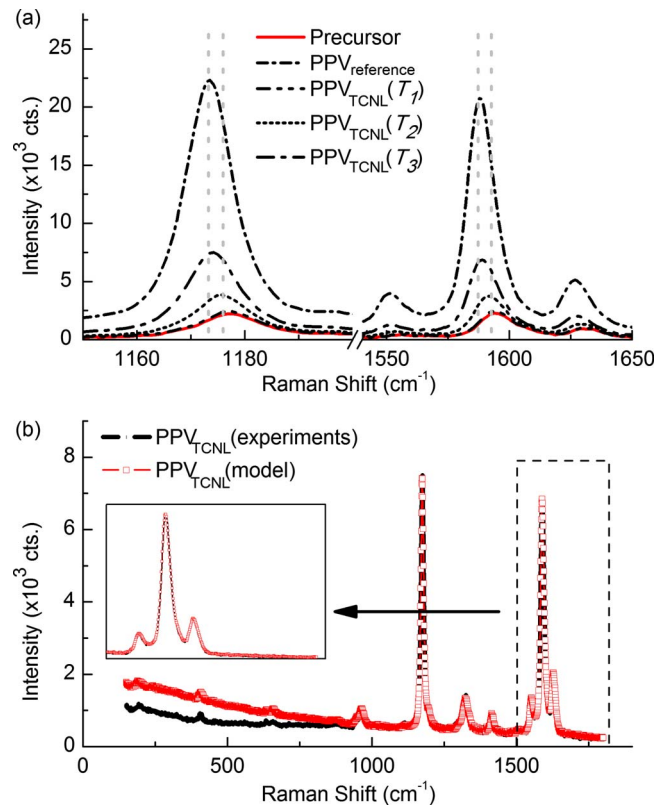

FIG. 3. (Color online) (a) Raman spectra as a function of the temperature used during TCNL, T_1=240 °C, T_2=280 °C, and T_3=320 °C, respectively. (b) Comparison between the Raman spectra obtained from the PPV$_{TCNL}$ pattern ($I_{PPV_{TCNL}}^{Experiment}$) and the combined Raman spectra obtained from Eq. (1) ($I_{PPV_{TCNL}}^{Model}$). Note that the continuum background is much lower in the TCNL sample than in the vacuum-annealed sample according to the model.

those of the precursor polymer and those of the PPV$_{reference}$ polymer. As the tip temperature used to perform TCNL increases, the Raman intensity of the written patterns increases and the peak positions shift to those of the PPV$_{reference}$ film.

In order to obtain more quantitative information on the quality and degree of thermochemical conversion, we modeled the TCNL modified film as composed of α% of precursor polymer and (100-α)% of PPV$_{reference}$. The Raman spectrum of the composite system may thus be a linear superposition of the spectra of the two constituents, namely precursor and PPV$_{reference}$ [reported in Figs. 2(a) and 2(b), respectively], as estimated by the following relationship:

$$I_{\mathrm{PPV_{TCNL}}}^{\mathrm{Model}} = \frac{\alpha}{100} \times (I_{\mathrm{precursor}} - I_{\mathrm{substrate}}) + \left(1 - \frac{\alpha}{100}\right)$$
$$\times (I_{\mathrm{PPVreference}} - I_{\mathrm{substrate}}). \qquad (1)$$

Figure 3(b) illustrates the the Raman spectra obtained from the TCNL pattern produced at 300 °C ($I_{\mathrm{PPV_{TCNL}}}^{\mathrm{Experiment}}$) and $I_{\mathrm{PPV_{TCNL}}}^{\mathrm{Model}}$ derived from Eq. (1). The free fitting parameter α was found by fitting $I_{\mathrm{PPV_{TCNL}}}^{\mathrm{Model}}$ to $I_{\mathrm{PPV_{TCNL}}}^{\mathrm{Experiment}}$ in the range $1500-1800$ cm^{-1}. This spectral region is far off the background signal caused by oxidation. With the blending ratio of 27% PPV$_{reference}$ and 73% precursor, the peak frequencies and intensity of $I_{\mathrm{PPV_{TCNL}}}^{\mathrm{Model}}$ are found to be perfectly overlapping in both intensity and peak-positions with $I_{\mathrm{PPV_{TCNL}}}^{\mathrm{Experiment}}$ in the considered frequency range. However, the broad background signal persistent at the head side is very different in the two cases. We speculate that this persistent difference could arise from partial oxidation of the PPV$_{reference}$ sample. In comparison with PPV$_{reference}$, the TCNL samples show a smaller background intensity at low frequencies, which suggests that the TCNL method may produce higher quality PPV samples. We attribute this improvement to the TCNL-specific geometry in which the temperature is increased locally at the tip-surface "sealed" contact. By using the above found parameter α=73%, we can estimate that out of the 1.4 μm thick precursor film, a precursor thickness of around 320 nm has been converted to the reference grade of PPV in a single application of TCNL at 320 °C. This thickness can be controlled by changing the tip temperature and contact time, which is an advantage of the TCNL process.

After our study had been completed, we became aware of a recent related work,[13] where the authors also used local heating to fabricate PPV nanostructures, but using a hot wire rather than an AFM tip. The present study shows high quality PPV nanostructures produced by TCNL in ambient conditions and confirmed via standard spectroscopic analysis.

In summary, PPV nanostructures have been made by TCNL, where PPV nanostructures were formed from a sulfonium salt precursor polymer by the thermal conversion in ambient conditions. The successful PPV conversion was verified by both Raman spectroscopy and fluorescence imaging. Furthermore, the dimension and thickness of the nanostructures can be controlled easily by varying the tip position and temperature. The resolution of the written nanostructures can be further improved by decreasing the thickness of the precursor film.[13] This state of the art nanopatterning of conjugated polymer, combined with the existing Millipede technology,[20] could facilitate the design and fabrications of future nanoelectronic, nanophotonic, and biosensing devices.

[1]D. D. C. Bradley, J. Phys. D: Appl. Phys. **20**, 1389 (1987).
[2]J. H. Burroughes, D. D. C. Bradley, A. R. Brown, R. N. Marks, K. Mackay, R. H. Friend, P. L. Burns, and A. B. Holmes, Nature (London) **347**, 539 (1990).
[3]H. Sirringhaus, T. Kawase, R. H. Friend, T. Shimoda, M. Inbasekaran, W. Wu, and E. P. Woo, Science **290**, 2123 (2000).
[4]M. Granstrom, K. Petritsch, A. C. Arias, A. Lux, M. R. Andersson, and R. H. Friend, Nature (London) **395**, 257 (1998).
[5]M. H. Yun, N. V. Myung, R. P. Vasquez, C. S. Lee, E. Menke, and R. M. Penner, Nano Lett. **4**, 419 (2004).
[6]J. Kameoka, D. Czaplewski, H. Q. Liu, and H. G. Craighead, J. Mater. Chem. **14**, 1503 (2004).
[7]E. Tekin, E. Holder, D. Kozodaev, and U. S. Schubert, Adv. Funct. Mater. **17**, 277 (2007).
[8]B. Dong, N. Lu, M. Zelsmann, N. Kehagias, H. Fuchs, C. M. S. Torres, and L. F. Chi, Adv. Funct. Mater. **16**, 1937 (2006).
[9]J. H. Lim and C. A. Mirkin, Adv. Mater. **14**, 1474 (2002).
[10]B. W. Maynor, S. F. Filocamo, M. W. Grinstaff, and J. Liu, J. Am. Chem. Soc. **124**, 522 (2002).
[11]E. Betzig and J. K. Trautman, Science **257**, 189 (1992).
[12]R. Riehn, A. Charas, J. Morgado, and F. Cacialli, Appl. Phys. Lett. **82**, 526 (2003).
[13]O. Fenwick, L. Bozec, D. Credgington, A. Hammiche, G. M. Lazzerini, Y. R. Silberberg, and F. Cacialli, Nat. Nanotechnol. **4**, 664 (2009).
[14]D. J. Lipomi, R. C. Chiechi, M. D. Dickey, and G. M. Whitesides, Nano Lett. **8**, 2100 (2008).
[15]R. Szoszkiewicz, T. Okada, S. C. Jones, T. D. Li, W. P. King, S. R. Marder, and E. Riedo, Nano Lett. **7**, 1064 (2007).
[16]D. B. Wang, R. Szoszkiewicz, M. Lucas, E. Riedo, T. Okada, S. C. Jones, S. R. Marder, J. Lee, and W. P. King, Appl. Phys. Lett. **91**, 243104 (2007).
[17]D. Wang, V. K. Kodali, W. D. Underwood, J. E. Jarvholm, T. Okada, S. C. Jones, M. Rumi, Z. Dai, W. P. King, S. R. Marder, J. E. Curtis, and E. Riedo, Adv. Funct. Mater. **19**, 3696 (2009).
[18]J. Lee, T. Beechem, T. L. Wright, B. A. Nelson, S. Graham, and W. P. King, J. Microelectromech. Syst. **15**, 1644 (2006).
[19]M. Granstrom, Synth. Met. **102**, 1042 (1999).
[20]P. Vettiger, G. Cross, M. Despont, U. Drechsler, U. Durig, B. Gotsmann, W. Haberle, M. A. Lantz, H. E. Rothuizen, R. Stutz, and G. K. Binnig, IEEE Trans. Nanotechnol. **1**, 39 (2002).